

## EFFECTS OF PYROLYSIS CONDITIONS ON COAL DEVOLATILIZATION

J. D. Freihaut and D. J. Seery  
United Technologies Research Center  
East Hartford, CT 06108

Phenomenological aspects of coal devolatilization are known to vary significantly with coal rank and the experimental conditions (1). Arrhenius rate parameters or volatile yields and product distributions can differ appreciably (2,3,4,5) for coals of similar rank depending on the experimental configuration. Differences in proposed chemical kinetic mechanisms undoubtedly account for part of the differences in reported rate parameters. However, experimentally associated variation of product yields and distributions and temperature sensitivities of global rates for similar coals implies that the observable path of the devolatilization process is the result of coupled chemical and transport processes. The physical characteristics of coal devolatilizing in a given set of conditions are also observed to vary significantly with chemical characteristics of the parent coal (6,7,8). And for a particular coal, the physical characteristics during devolatilization are observed to be a function of the conditions of heating (9,10,11,12). Such associations also imply that observable behavior during coal devolatilization is a result of the coupling between the chemical nature of the parent coal and particular conditions of the experiment.

Polycyclic aromatic hydrocarbon species represent a major fraction of the volatile yields obtained from a wide range of coals. The overwhelming majority of these species are condensible under conditions of normal temperature and pressure and are operationally referred to as coal tars. Tar yields obtained from the devolatilization of coal are sensitive functions of the chemical characteristics of the parent coal and the conditions of devolatilization. As tar yields for a particular coal are changed by variation of either the chemical characteristics of the parent coal or conditions of devolatilization, the yield structure and characteristics of the products are also changed.

The purpose of this communication is to demonstrate that progress in understanding the relative importance of chemical and physical factors in coal devolatilization is linked to progress in understanding the formation, evolution and secondary reactions of PAH species which are apparently formed within the coal particle very early in the devolatilization process. More specifically, the objectives are to demonstrate the significance of the tar formation and evolution phase of coal devolatilization in determining:

1. the yield structure of volatile products from a range of coals;
2. the change in yield structure with conditions of devolatilization;
3. the degree of coupling between chemical and physical phenomena during the main phase of mass release.

## Experimental

Two experimental techniques were employed in obtaining the results - a heated grid apparatus and a flash lamp chamber. Figure 1 shows the heated grid and associated control and monitoring connections. Since the power supply driving the grid is programmable, the heating rate of the grid can be controlled by interfacing the power supply to microprocesses or circuitry. Programmed heating rates of  $< 10^{\circ}\text{C}/\text{sec}$  to  $10^3 \text{ }^{\circ}\text{C}/\text{sec}$  are available by use of this technique. The heated grid cell is interfaced to an infrared gas cell. The cell is coupled to an FT-IR instrument to allow immediate analysis of low molecular weight volatiles. Details of the operation of the heated grid (screen preparation, sample loading, thermocouple measurements) are given elsewhere (13,14).

The grid technique, as employed in this laboratory, cannot be used with particles less than  $\sim 70 \mu\text{m}$  and heating rates are practically limited to upper values  $\sim 10^3 \text{ }^{\circ}\text{C}/\text{sec}$ . A different technique is needed to heat particles in the  $1\text{-}70 \mu\text{m}$  range at programmed heating rates of  $10^5 \text{ }^{\circ}\text{C}/\text{sec}$ . To obtain these conditions of large thermal flux/particle diameter ratios a flash lamp assembly replaces the heated grid chamber of Fig. 1. In this technique the inside of a pyrex or quartz tube is dusted with the coal. The tubes are  $2.5 \text{ cm}$  in diameter and  $\sim 10 \text{ cm}$  long and sealed at one end. The coated reactor tube is placed inside a helical Xenon flash coil. The flash intensity delivered to the reactor tube is varied by the energy stored in the  $1125 \mu\text{f}$  capacitor bank attached to the flash lamp. Since the total energy stored in the capacitor system is  $\frac{1}{2}CV^2$ , an increase in voltage from  $1.5$  to  $2.5 \text{ kV}$  represented approximately a 2.8 increase in flash energy output. Since the discharge time and reactor geometry remain constant the increase in programmed voltage represents an increase of 2.8 in radiation flux delivered to the reactor chamber. Pyrex reactor chambers were employed in most tests to avoid UV-induced secondary reactions. Sample sizes range in value from  $3\text{-}10 \text{ mg}$ .

## Coal Characteristics

The location of the samples on a H/C vs. O/C plot are shown in Fig. 2. Figure 3 displays changes in functional group absorption characteristics as a function of rank. In general, an increase in rank is associated with an increase in the resolution of the aromatic  $\text{-H}$  bending ( $680\text{-}920 \text{ cm}^{-1}$  region) and aromatic  $\text{-H}$  stretching ( $3000\text{-}3100 \text{ cm}^{-1}$ ), a decrease in the hydroxyl  $\text{-H}$  associated absorption in the  $3100\text{-}3600 \text{ cm}^{-1}$  region, and a maximum in aliphatic  $\text{-H}$  absorption modes  $2600\text{-}3000 \text{ cm}^{-1}$  and  $\sim 1400 \text{ cm}^{-1}$  regions for hv bituminous coals. It should be noted that these functional group spectra were obtained by artificially establishing a baseline. A chord is drawn through the local spectra absorption minima at  $\sim 3600 \text{ cm}^{-1}$  and  $2000 \text{ cm}^{-1}$ . The so-called "background" absorption beneath this chord line and the raw spectra, zero absorbance line is subtracted, leaving the chord line as the new zero absorbance line. Although this is a convenient method for comparing changes in functional group appearance, it ignores the substantial changes in optical density of coal with rank.

Figure 4 shows the background absorption subtracted in this manner as a function of carbon percentage content of the coal samples. Figure 5 shows the remaining

integrated absorption area ( $400-4000\text{ cm}^{-1}$ ). This is the absorption area assumed to be associated with specific functional group characteristics, the area between the chord drawn baseline and the absorption curve. Inspection of Figs. 4 and 5 indicates that as the functional group absorption characteristics of coal decrease, its amorphous background absorption sharply increases. The underlying cause of the background absorption are not well understood. Some investigators relate such optical attenuation to particle scattering effects in the halide matrix (15,16). Others attribute the bulk of this absorption to photoabsorption by condensed aromatic ring species in the coal sample (17,18,19,20). The greater the aromaticity of the coal the greater the photoabsorption effect, that is, the greater the background absorption. The two phenomena are undoubtedly coupled via the complex refractive index for a particular coal relative to the halide matrix. The strength of coupling remains to be quantified. Overall, the total optical density of a coal is a strong function of rank as measured by  $\%C(\text{daf})$ .

Within the hv bituminous coals, the Western bituminous coals, although similar in elemental composition to some interior and Appalachian province coals, show absorption characteristics indicating a lower degree of aromaticity. This is indicated by the ill resolved aromatic -H absorption modes ( $680-920\text{ cm}^{-1}$  and  $3000-3100\text{ cm}^{-1}$ ) and the lower background absorption than the other bituminous coals.

As noted below, the degree of aromatic ring condensation has a substantial influence on the maximum PAH yields obtainable from a coal as well as the sensitivity of the yield to changes in pyrolysis conditions.

#### Tar Evolution: Coupling Between Coal Characteristics and Moderate Heating Rates

Figure 6 displays the mass fraction of dry coal evolved as volatiles for the range of coals investigated and at the heating conditions indicated. At these conditions, total yield is essentially independent of rank characteristics through high volatile bituminous coals. However, as Figs. 7 and 8 indicate, the tar yield is a sensitive function of rank characteristics of a coal. Appalachian and Interior province high volatile bituminous coals give highest yields of tars and, with the exception of a medium volatile bituminous coal, display the greatest fraction of volatiles evolved as condensable PAH species. Figure 9 indicates the variation in tar yields with heating conditions for a Western bituminous coal. There is little change in volatile yields with heating conditions for final temperatures beyond  $700^{\circ}\text{C}$  in the time period of this experiment. However, the fraction of volatiles evolved as tar decreases significantly with changes in programmed heating rate from  $150^{\circ}\text{C}/\text{sec}$  to  $\sim 1000^{\circ}\text{C}/\text{sec}$ . Tar yields from Appalachian and Interior province bituminous coals yield tar species which are much less sensitive to changes in programmed heating rates. Such coals show less than 10% change in tar yield with changes in programmed heating rate in the  $100-1000^{\circ}\text{C}/\text{sec}$  range, whereas tar yields from sub-bituminous and Western bituminous coals can vary by as much as 50% over this range. The aromaticity, and, consequently the chemical and thermal stability of the mix of molecular components in the parent coal has a great deal of influence on the tar evolution properties of a coal.

The tar evolution potential of a coal is also observed to have a significant influence on the temperature trajectory of the heated grid in immediate contact with the

coal sample. Figure 10 shows the effect which tar evolution properties of a coal can have on a programmed temperature trajectory in low pressure conditions.

Figure 11 shows the time resolved associated between the low pressure evolution of the tar component of the volatiles and the warp in the programmed temperature trajectory. Figures 9 and 11 indicate that in low ambient pressure conditions the formation and evolution of PAH species precedes significant light gas evolution. To verify the relative release times, high speed films of the tar release process were made.

Frame-by-frame inspection of these films were compared to the rapid scan infrared data and real time pressure and temperature data. For the coals examined in this manner.

1. The initial temperature deviations are closely associated with the tar formation and release.
2. The onset of the tar release precedes the onset of the major light gas release.
3. The light gas evolution occurs mainly in the secondary temperature rise.
4. Rocky Mt. province high volatile bituminous coals displayed more overlap in the tar and light gas evolution than the Appalachian province high volatile bituminous coals.
5. Lower rank coals gave increasingly greater degrees of overlap between the light gas and tar evolution phases of devolatilization.

#### Dependence of Coal Nitrogen Evolution on Tar Evolution Characteristics

For final temperature  $< 1000^{\circ}\text{C}$  and heating rates  $10^2\text{-}10^3$   $^{\circ}\text{C}/\text{sec}$ , the distribution of coal nitrogen in the tar, char or light gases produced by devolatilization is dependent on the chemical characteristics of the coal in a manner analogous to the distribution of coal mass as tar, char or light gas. An increase in the tar fraction of the volatiles with increase in aromaticity of the parent coal results in a proportionate increase in coal nitrogen in the tar. A decrease in tar yield for a particular coal by increases in apparent heating rate results in a proportionate decrease in coal nitrogen evolved as tar. As the tar yield decreases, the tar nitrogen is primarily evolved as HCN. The coupling between the tar and gaseous evolution of the coal nitrogen and the dependence on aromaticity of the parent coal are illustrated by Figs. 12-14. Mass balance details and distributions for other coals are given elsewhere (21).

#### Effect of Low and High Programmed Heating Rates

Table I displays the sizable variation in solids and tar yields with programmed conditions of heating for two hv bituminous coals. Inspection of Table I indicates tar

TABLE 1  
 VARIATION OF CHAR AND TAR YIELDS WITH HEATING RATES

Coal	Programmed Heating Rate ( $^{\circ}\text{C}/\text{sec}$ )	Wt% Char/Soot	Wt% Tar (THF Soluble)	Final Temp. $^{\circ}\text{C}$
Utah Bit.	1	63	10	800
	$10^2$	53	30	800
	$10^3$	51	17	900
	$+10^5^*$	$76^{\dagger}$	14	**
Ken Bit.	1	62	15	800
	$10^2$	52	39	800
	$10^3$	50	35	900
	$+10^5^*$	$61^{\dagger}$	21	**

\* Flash lamp operated at 2.5 kV-1125  $\mu\text{f}$  discharge conditions, 2 msec flash pulse  
 Particle size range of coal -140+325 mesh in all runs.

\*\* Not known.

$^{\dagger}$ A fraction of non-THF soluble tars has soot-like physical characteristics.

yields and char yields are minimized for hv Bit coals in moderate heating conditions and low pressure conditions. Very low heating rates and very high heating rates have the effect of decreasing tar yields while increasing solids yields, either in the form of char or a combination of char and soot. Light gas yields reflect the thermal flux conditions in the tar formation and evolution stages.

### Summary and Discussion of Results

The formation and evolution of PAH species in coal devolatilization is observed to be a sensitive function of the mix of molecular species present in the parent coal. Through high volatile bituminous coals and within moderate heating conditions, PAH yields increase with apparent aromaticity of the coal. Those coals having the greater aromaticity, as indicated by infrared absorption characteristics, give consistently greater tar yields than less aromatic samples. Such coals also show less variation in tar yields with changes in heating rate. For moderate heating rates to final temperatures less than  $1000^{\circ}\text{C}$ , the coal nitrogen evolution mirrors the parent coal evolution as char, tar or light gas species on a mass fraction basis. Heating rates of  $1^{\circ}\text{C}/\text{sec}$  or less are observed to lower tar yields of bituminous coals while increasing char and light gas yields. On the other hand, programmed heating rates of  $10^5$ - $10^6$   $^{\circ}\text{C}/\text{sec}$  also result in a decrease in tar yields with an increase in solid species products. A fraction of these solids appear to be soot particles. Gaseous yields of coals subjected to such high thermal fluxes show  $\text{C}_2\text{H}_2$ ,  $\text{CO}$ ,  $\text{CH}_4$ ,  $\text{HCN}$ ,  $\text{C}_2\text{H}_4$  and polyacetylenes as the predominant gas phase species.

Not only do tar yields vary with heating conditions but evolution times vary significantly as well. Tar formation and evolution times are observed to be of the order of several milliseconds in the highest programmed heating rates employed to fraction of seconds to seconds in moderate heating rate conditions, and hundreds of seconds in the lowest heating rates employed. Formation of polycyclic aromatic species appears to begin at relatively low temperature, that is in the  $300$ - $475^{\circ}\text{C}$  temperature range. The ultimate tar yield then appears to be a complex function of heat and mass transfer parameters as well as chemical characteristics of these primary tars. For hv Bit coals and lower ranks, the more aromatic the primary tars, the less secondary chemical reactions influence observable behavior. For these coals, the initial mass loss of the coal is likely heat and mass transport limited. For higher rank coals, the primary tars are likely to be of such molecular weights and dimension that secondary char-forming reactions will become competitive with the tar evolution process. In view of such considerations, the wide variation in reported results reflect the coupled effects of intrinsic and extrinsic parameters on primary PAH formation and evolution.

Low heating rates allow secondary char-forming reactions of tars to take place within the coal particle. Very high heating rates introduce secondary cracking and ring condensation reactions of primary tars as they evolve. The susceptibility of primary tars to undergo char-forming or cracking reactions is a function of chemical characteristics of the primary tars. As noted in the Introduction the development of a comprehensive model of coal devolatilization/pyrolysis for a single rank of coal in a range of conditions or a range of coals in a single condition is contingent upon fundamental studies of the formation and evolution of primary PAH species.

## REFERENCES

1. Howard, J. B., "Fundamentals of Coal Pyrolysis and Hydropyrolysis," Chemistry of Coal Utilization, 2nd Supp. Volume, M. A. Elliott (Editor), Wiley - Interscience, New York, 665 (1981).
2. Solomon, P. R. and Colket, M. B., Seventeenth Symposium (International) on Combustion, The Combustion Institute, Pittsburgh, PA, 131 (1979).
3. Anthony, D. B., Howard, J. B., Hottel, H. C. and Meisner, H. P., Fifteenth Symposium (International) on Combustion, The Combustion Institute, Pittsburgh, PA 1303 (1975).
4. Tyler, R. J., Fuel, 59, 218 (1980).
5. Kobayashi, H, Howard, J. B. and Sarofim, A. F., Sixteenth Symposium (International) on Combustion, The Combustion Institute, Pittsburgh, PA 411 (1977).
6. Brown, H. R., Hesp, W. R., and Waters, P. L., J. Inst. Fuel, 130 (1964).
7. Cameron, A. R. and Botham, J. C., Coal Science, 55, 564 (1966).
8. Habermehl, D., Orywal, F., and Beyer, Hans-Dieter, "Plastic Properties of Coal," Chemistry of Coal Utilization and Supp. Volume, M. A. Elliott (Editor), Wiley-Interscience, New York, 317 (1981).
9. Gryaznov, N. S., Coke Chem. USSR, 1, 5 (1962).
10. Van Krewlen, D. W., Huntjens, F. J., and Dormans, H. N. M., Fuel, 35, 462 (1956).
11. Kreulen, D. J. W., Fuel, 29, 112 (1950).
12. Nadziakiewicz, J., Fuel, 37, 361 (1958).
13. Freihaut, J. D., Zabielski, M. F. and Seery, D. J., Amer. Chem. Soc. Div. of Fuel Chem., 27, No. 2, 89 (1982).
14. Freihaut, J. D., Zabielski, M. F. and Seery, D. J. Nineteenth Symposium (International) on Combustion, The Combustion Institute, Pittsburgh, PA, 1159 (1982).
15. Bergmann, G., Husk, G., Karwell, J. and Luter, H., Brennstoff Chem., 35, 175 (1954).
16. Duyckaerts, G., The Analyst, 84, 201 (1959).
17. Friedel, R. A., Fuel, 38, 541 (1959).

18. Kmetko, E. A. *Phys. Rev.*, 82, 456 (1951).
19. Brown, J. K., Jr. *Chem. Soc.*, 744 (1955).
20. Friedel, R. A., and Queiser, J. A., Jr. *Anal. Chem.*, 28, 22 (1956).
21. Freihaut, J. D., and Seery, D. J., *Am. Chem. Soc. Div. of Fuel. Chem.*, 26, No. 3, 18 (1981).

#### ACKNOWLEDGMENTS

The authors express their gratitude to G. Wagner and D. Santos for their technical expertise in performing this investigation. Part of this work was sponsored by DOE Contract DE-AC21-81MC16221.

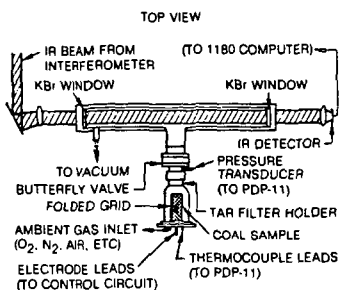


FIG. 1. Schematic of coal/devolatilization apparatus.

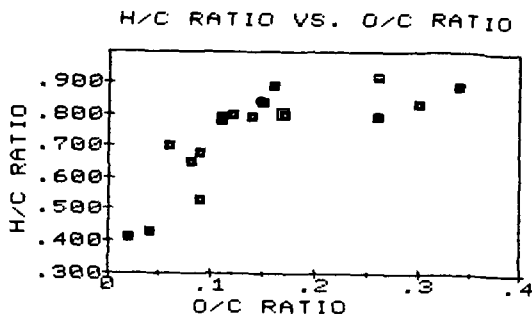


Fig. 2. Sample locations on coalification band.

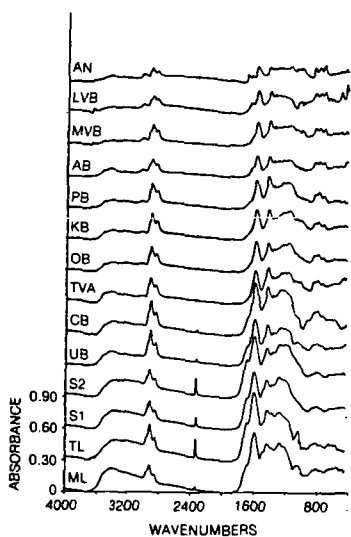


FIG. 3. Infrared absorption spectra of coals. Mineral matter subtracted. Baseline corrected.

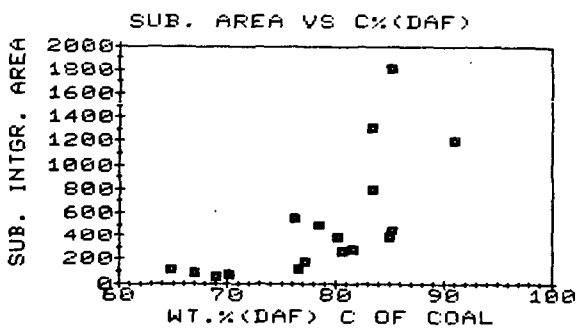


Fig. 4. Integrated area ( $400-4000\text{ cm}^{-1}$ ) beneath chord drawn through tangent points at  $3600\text{ cm}^{-1}$  and zero absorbance line: C fraction calculated dry and free (DAF) basis.

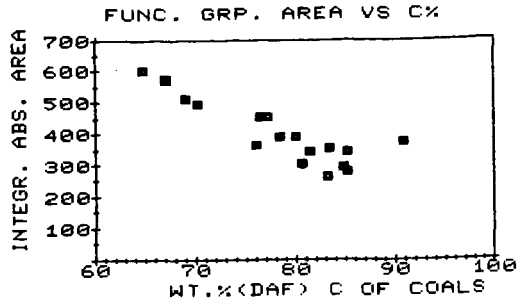


Fig. 5. Integrated area (400-4000  $\text{cm}^{-1}$ ) between chord baseline and absorption curve.

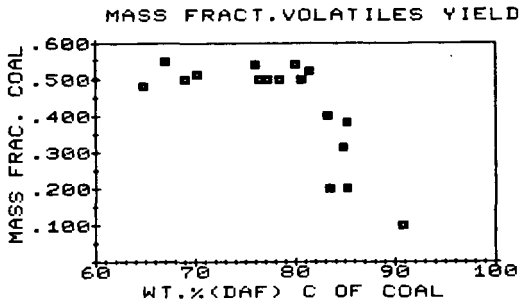


Fig. 6. Programmed heating rate  $500^{\circ}\text{C}/\text{sec}$ ; final temperature  $900^{\circ}\text{C}$ ; see Ref. 13, 14 for sample loading conditions; dry sample used as basis of calculation; ambient pressure  $\sim 10^{-2}$  torr;  $-140+325$  mesh particles.

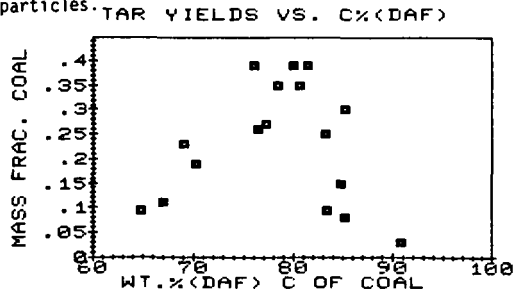


Fig. 7. Conditions as noted in Fig. 6.

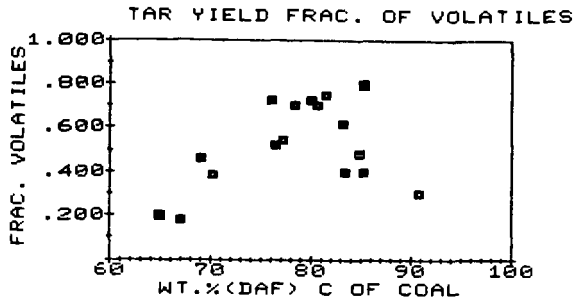


Fig. 8. Fraction of total volatiles evolved as PAH species.

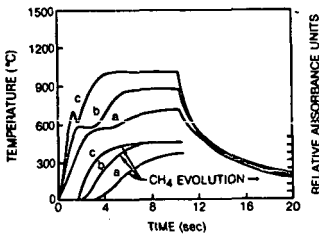


Fig. 9. Time resolved temperature and  $CH_4$  evolution data for Rocky Mt. bituminous coal; a = 55.4% char; 30% tar; b = 52.6% Char, 24.0% tar; c = 51.3% char, 17.0%.

#### VARIATION OF THERMAL LOADING WITH RANK — CATS SYSTEM

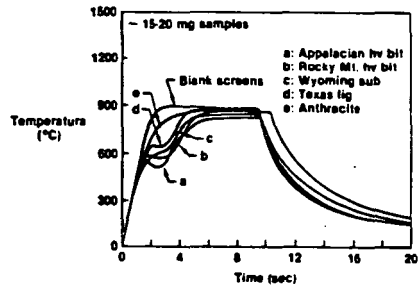


Fig. 10 a = 39% tar; b = 24% tar; c = 20% tar; d = 11% tar; e = 3% tar; see Ref. 13, 14 for loading conditions and thermocouple placement.

### TAR AND LIGHT HYDROCARBON YIELDS

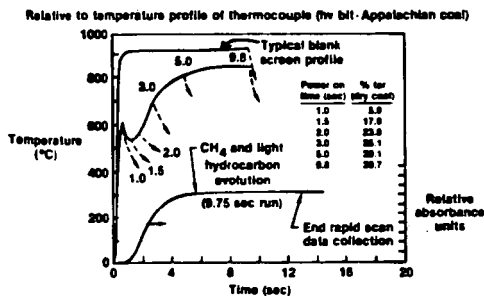


Fig. 11. Effect of tar release on temperature profile; see Ref. 13 and 14 for leading technique and thermocouple placement.

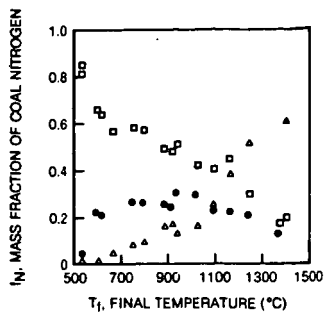


Fig. 12. Nitrogen distribution in devolatilization products; Rocky Mt. bituminous coal;  $\square$  = char;  $\bullet$  = tar;  $\Delta$  HCN.

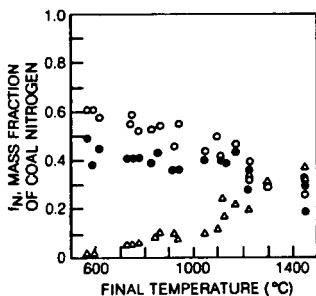


Fig. 13 Nitrogen distribution in devolatilization products; Appalachian Province bituminous coal;  $\circ$  = char,  $\bullet$  = tar,  $\Delta$  = HCN.

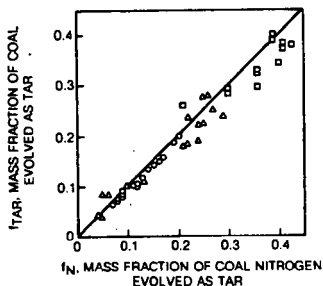


Fig. 14. Mass fraction parity between evolved tar and coal nitrogen as tar;  $\Delta$  = Rocky Mt. Bit;  $\square$  = Appalachian Bit;  $\circ$  = Subbituminous.